

Supporting Information

**Nitroprusside as a promising building block to assemble organic-inorganic
hybrid for thermo-responsive switching material**

*Rong-Guan Qiu,^a Xiao-Xian Chen,^a Rui-Kang Huang,^a Dong-Dong Zhou,^a Wei-Jian Xu,^{*a,b} Wei-Xiong
Zhang^{*a} and Xiao-Ming Chen^a*

^a MOE Key Laboratory of Bioinorganic and Synthetic Chemistry, School of Chemistry, Sun Yat-Sen University, Guangzhou, 510275, P. R. China.

^b Department of Chemistry & CICECO-Aveiro Institute of Materials, University of Aveiro, 3810-193 Aveiro, Portugal.

Experimental

Synthesis

All chemicals were commercially available and used without further purification. The red block crystals of **1** were obtained by slow evaporation of an aqueous solution containing 2.95 g K₂[Fe(CN)₅(NO)] and 0.88 g (Me₂NH₂)Cl at room temperature for several days. Yield: 86% based on K₂[Fe(CN)₅(NO)]. Elemental analysis, calcd (%) for **1** (C₇H₈N₇OF₂K): C, 27.92; N, 32.56; H, 2.68. Found, C, 28.35; N, 32.15; H, 2.69.

X-ray Crystallographic Analysis

The *in-situ* variable-temperature single-crystal diffraction intensities data were collected on an Agilent SuperNova, with AtlasS2 diffractometer (Cu K_{α} , $\lambda = 1.54184 \text{ \AA}$) in a temperature range of 100–385 K. The *CrysAlis PRO* software package was used for data collection, cell refinement and data reduction. Using Olex² program, the structures were solved by using Intrinsic Phasing with the SHELXT structure solution program and using full-matrix least-squares method with the SHELXL refinement program.^{S1, S2} The structures of LTP were refined using a racemic twinning matrix [-1 0 0 0 -1 0 0 0 -1] and BASF factor. Non-hydrogen atoms were refined anisotropically and the positions of the hydrogen atoms were generated geometrically. Crystallographic data and structural refinements are summarized in Table S1. Powder X-ray diffraction (PXRD) patterns (Cu K_{α} , $\lambda = 1.54184 \text{ \AA}$) were collected on Bruker Advance D8 DA VANC_I θ -2 θ diffractometer.

Elemental analysis

Elemental (C, H, and N) analyses were performed on a Perkin-Elmer Vario EL elemental analyzer with as-synthesized samples.

Thermal Analysis

Thermogravimetric analysis (TGA) was carried out on a TA Q50 system with a heating rate of 10 K min⁻¹ under a nitrogen atmosphere. Differential scanning calorimetry (DSC) was carried out on a TA DSC Q2000 instrument under a nitrogen atmosphere in aluminum crucibles with heating and cooling rates of 10 K min⁻¹ from 200 to 420 K.

Dielectric measurements

The dielectric measurement was carried on a Keysight E4990A impedance analyzer at 10 frequencies from 9978.32 Hz to 147612.9 Hz, with an applied voltage of 1.0 V and a temperature sweeping rate of 3 K min⁻¹ approximately in the range of 80–400 K in a Mercury iTC cryogenic environment controller of Oxford Instrument. The powder sample of **1** was ground and pressed into tablets under a pressure around 2 GPa. The capacitor was made by painting the two faces of tablet pieces with silver conducting paste and using gold wires as the electrodes.

SHG Measurement

Variable-temperature SHG experiment was executed by Kurtz-Perry powder SHG test using an Nd:YAG laser (1064 nm) with input pulse of 570 V under a programmable cryogenic cooling system. Before the experiment, dark red polycrystalline samples of **1** were screened into 60 and 70 meshes by standard sieves. The value of nonlinear optical coefficient for **1** has been determined by comparison with a potassium dihydrogen phosphate (KDP) reference.

Table S1. Crystal data and structure refinement parameters for **1** at LTP and HTP.

Compound	(Me ₂ NH ₂)[KFe(CN) ₅ (NO)] (1)											
Phase	LTP							HTP				
Crystal system	orthorhombic							orthorhombic				
Space group	<i>P</i> 2 ₁ 2 ₁ 2 ₁							<i>P</i> nma				
Temperature (K)	100(2)	150(2)	200(2)	220(2)	240(2)	260(2)	280(2)	305(2)	325(2)	345(2)	365(2)	385(2)
<i>a</i> (Å)	9.8433(1)	9.9126(1)	9.9983(1)	10.0402(1)	10.0838(1)	10.1350(2)	10.2018(2)	10.3262(4)	10.3494(6)	10.3809(8)	10.3982(8)	10.4242(1)
<i>b</i> (Å)	8.5320(1)	8.5286(1)	8.5234(1)	8.5197(1)	8.5150(1)	8.5134(1)	8.5037(2)	8.4855(3)	8.4866(5)	8.4936(7)	8.5036(7)	8.5078(8)
<i>c</i> (Å)	14.8241(2)	14.8615(2)	14.8981(2)	14.9130(2)	14.9235(2)	14.9364(3)	14.9480(4)	14.9627(5)	14.9745(8)	14.9835(9)	15.0131(1)	15.0275(4)
<i>V</i> (Å ³)	1244.97(3)	1256.40(3)	1269.61(3)	1275.65(3)	1281.38(3)	1288.76(4)	1296.78(6)	1311.08(8)	1315.23(3)	1321.11(7)	1327.49(8)	1332.7(2)
<i>Z</i>	4	4	4	4	4	4	4	4	4	4	4	
μ (mm ⁻¹)	12.707	12.591	12.460	12.401	12.346	12.275	12.199	12.066	12.028	11.975	11.917	11.870
<i>F</i> ₀₀₀	608.0	608.0	608.0	608.0	608.0	608.0	608.0	608.0	608.0	608.0	608.0	608
<i>R</i> _{int}	0.0496	0.0504	0.0502	0.0525	0.0578	0.0551	0.0678	0.0551	0.0597	0.0772	0.0745	0.0908
Completeness (%)	100	100	100	100	100	100	100	99	99	99	99	99
Reflns. collected	6766	6878	6993	7066	7084	7129	6744	4061	4084	4017	3384	3465
Independent reflns.	2469	2491	2516	2530	2543	2559	2324	1391	1394	1398	1272	1278
<i>R</i> ₁ ^a [<i>I</i> > 2σ(<i>I</i>)]	0.0373	0.0373	0.0373	0.0386	0.0415	0.0421	0.0516	0.0489	0.0531	0.0638	0.0621	0.0673
<i>wR</i> ₂ ^b [<i>I</i> > 2σ(<i>I</i>)]	0.0974	0.0975	0.0982	0.1015	0.1080	0.1091	0.1343	0.1338	0.1445	0.1839	0.1702	0.1806
<i>R</i> ₁ ^a (all data)	0.0376	0.0375	0.0377	0.0390	0.0425	0.0429	0.0536	0.0500	0.0543	0.0668	0.0694	0.0903
<i>wR</i> ₂ ^b (all data)	0.0976	0.0978	0.0987	0.1019	0.1095	0.1107	0.1380	0.1358	0.1470	0.1885	0.1846	0.2440
GOF	1.070	1.048	1.048	1.028	1.052	1.038	1.081	1.036	1.035	1.106	1.110	1.179
BASF	0.237(8)	0.230(8)	0.222(8)	0.228(8)	0.223(9)	0.227(9)	0.24(1)	/	/	/	/	/

^a*R*₁ = Σ||*F*_o| - |*F*_c|| / Σ|*F*_o|; ^b*wR*₂ = [Σ*w*(*F*_o² - *F*_c²)² / Σ*w*(*F*_o²)²]^{1/2}.

Table S2. Hydrogen bond lengths for **1**.

LTP							
T (K)	100(2)	150(2)	200(2)	220(2)	240(2)	260(2)	280(2)
$d(\text{N1-H}\cdots\text{N2})$ (Å)	2.932(5)	2.928(5)	2.927(6)	2.926(6)	2.920(6)	2.921(6)	2.914(8)
$d(\text{N1-H}\cdots\text{N3D})$ (Å)	3.134(5)	3.114(5)	3.090(5)	3.080(6)	3.062(6)	3.047(6)	3.033(8)
Symmetry code: D, $(x, -1+y, z)$							
HTP							
T (K)	305(2)	325(2)	345(2)	365(2)	385(2)		
$d(\text{N1-H}\cdots\text{N2})$ (Å)	2.926(4)	2.929(4)	2.934(7)	2.944(7)	2.969(1)		

Table S3. Selected bond lengths for **1**.

LTP							
T (K)	100(2)	150(2)	200(2)	220(2)	240(2)	260(2)	280(2)
$d(\text{Fe1-N7})$ (Å)	1.659(3)	1.659(3)	1.657(3)	1.653(3)	1.649(4)	1.652(4)	1.651(5)
HTP							
T (K)	305(2)	325(2)	345(2)	365(2)	385(2)		
$d(\text{Fe1-N5})$ (Å)	1.658(3)	1.657(4)	1.653(5)	1.652(5)	1.641(8)		

Table S4. The thermal expansion coefficients for **1**.

	Principal axes	α or β_v ($\times 10^{-6} \text{ K}^{-1}$)	direction		
			<i>a</i>	<i>b</i>	<i>c</i>
LTP	X_1	-17(2)	0	-1	0
	X_2	+47(1)	0	0	1
	X_3	+197(13)	1	0	0
	V	+230(11)			
HTP	X_1	+36(3)	0	-1	0
	X_2	+56(3)	0	0	1
	X_3	+119(2)	1	0	0
	V	+213(6)			

α and β_v represent axial and volumetric thermal expansion coefficients, respectively.

Table S5. Some typical hybrid/molecule-based NLO-switching materials.

Compounds	Dimensionality	T_c (K)	Phase Transition	Ref.
$[(DPA)(18C6)](ClO_4)$	0D	214	$P2_12_12_1 \leftrightarrow Pnma$	[S3]
$[(C_5H_{10})(CH_3)NH](H_2O)(18C6)(ClO_4)$	0D	260	$Pn2_1a \leftrightarrow Cmc2_1$	[S4]
$(H_2dabcoCl_2)[FeCl_3(H_2O)_3]$	0D	280	$P2_12_12_1 \leftrightarrow Pnma$	[S5]
$[(CH_3)_3S][MBr_4]$ (M = Cd, Mn and Zn)	0D	315	$P2_12_12_1 \leftrightarrow Pnma$	[S6]
$(CH_3C(NH_2)_2)(ClO_4)$	0D	320	$P2_1 \leftrightarrow Pm-3m$	[S7]
$(C_4H_{16}N_3)[BiBr_6]$	0D	335	$P2_12_12_1 \leftrightarrow Pnnm$	[S8]
Bis(imidazolium) L-tartrate	0D	352	$P2_1 \leftrightarrow P2_12_12_1$	[S9]
$NH_4[(CH_3)_4N]SO_4 \cdot H_2O$	1D	204	$Pna2_1 \leftrightarrow Pnma$	[S10]
$(C_6H_{14}N)_2[SbCl_5]$	1D	335	$P2_12_12_1 \leftrightarrow Pnma$	[S11]
$[NH_3(CH_2)_5NH_3][SbCl_5]$	1D	365	$P2_12_12_1 \leftrightarrow Pnma$	[S12]
$(C_6H_{11}NH_3)_2[CdCl_4]$	1D	367	$Cmc2_1 \leftrightarrow I222$	[S13]
$(C_5H_{12}N)[SnCl_3]$	1D	371	$P2_12_12_1 \leftrightarrow P2_12_12_1$	[S14]
$(C_3H_4NS)_2\{(H_3O)[Co(CN)_6]\}$	2D	230	$Pca2_1 \leftrightarrow Pna2_1$	[S15]
$(C_4H_9NH_3)_2(CH_3NH_3)_2[Pb_3Br_{10}]$	2D	315	$Cmc2_1 \leftrightarrow Cmca$	[S16]
$(cyclohexylaminium)_2[PbBr_4]$	2D	360	$Cmc2_1 \leftrightarrow Cmca$	[S17]
$(C_4H_9NH_3)_2CsPb_2Br_7$	2D	412	$Cmc2_1 \leftrightarrow Cmca$	[S18]
$(benzylammonium)_2[PbCl_4]$	2D	438	$Cmc2_1 \leftrightarrow Cmca$	[S19]
$(Me_2NH_2)[KFe(CN)_5(NO)]$	3D	295	$P2_12_12_1 \leftrightarrow Pnma$	(This work)
$[Et_3(CH_2OCH_3)P][Mn(N(CN)_2)_3]$	3D	333	$P2_12_12_1 \leftrightarrow I4_1/amd$	[S20]
$[Et_3(CH_3CH_2CH_2)P][Cd(N(CN)_2)_3]$	3D	386	$P2_12_12_1 \leftrightarrow Ibam$	[S21]

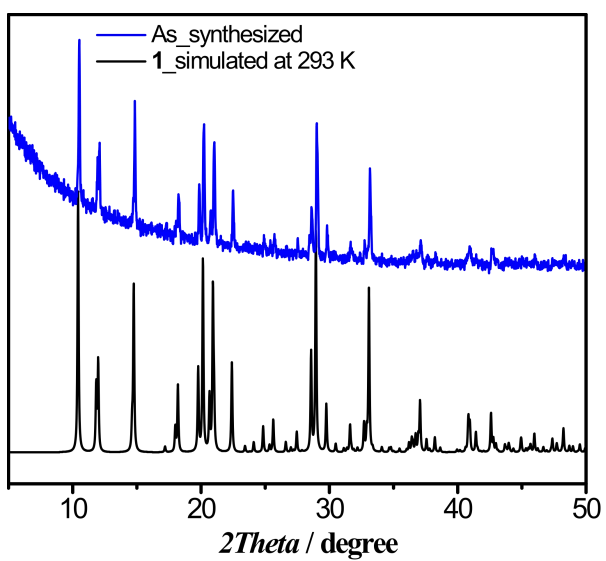


Figure S1. The PXRD patterns confirmed the phase purity of the as-synthesized sample **1**.

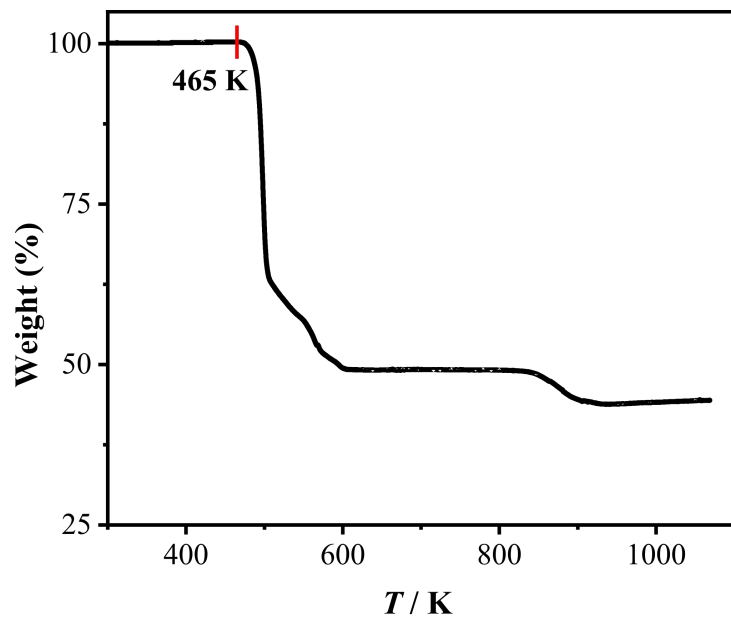


Figure S2. TG profile of **1**.

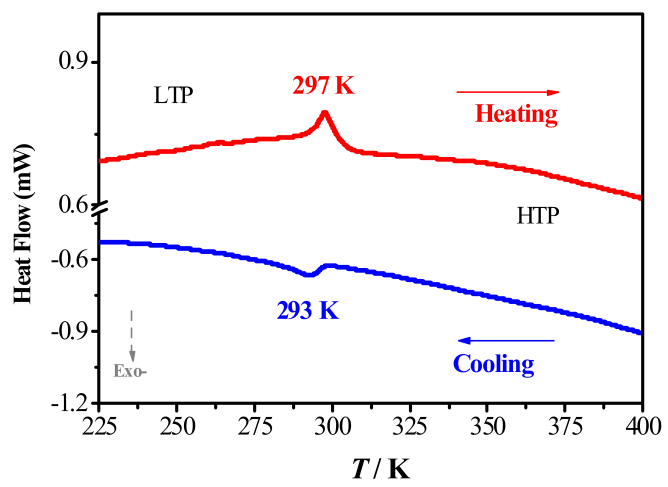


Figure S3. DSC curves of **1**.

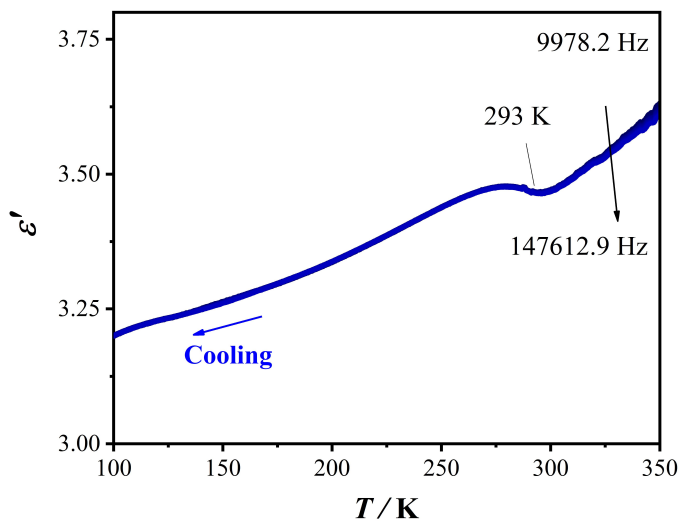


Figure S4. Temperature dependence of ϵ' of **1** measured on the powder sample at different frequencies (cooling mode).

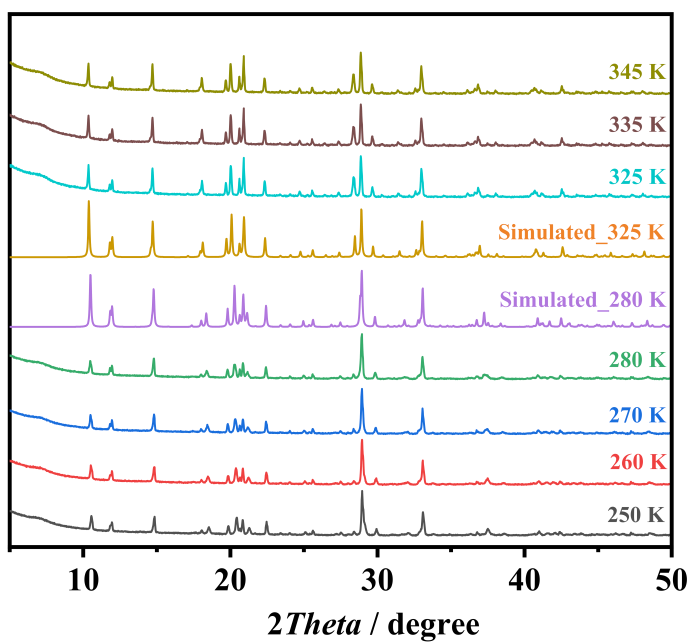


Figure S5. The variable-temperature powder X-ray diffraction patterns of **1**.

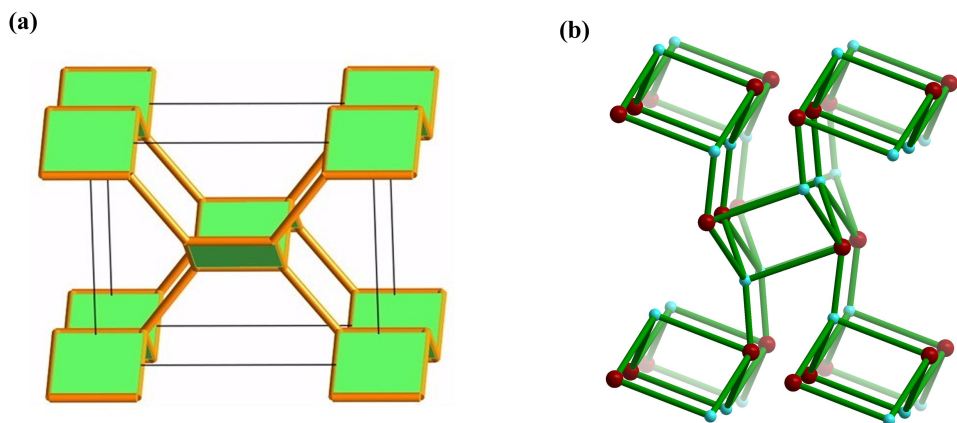


Figure S6. The sra topology for **1**. For more information, see references:
<http://rcsr.net/nets/sra>, *CrystEngComm* 2004, **6**, 377-395, *J. Am. Chem. Soc.* 2005, **127**, 1504-1518.

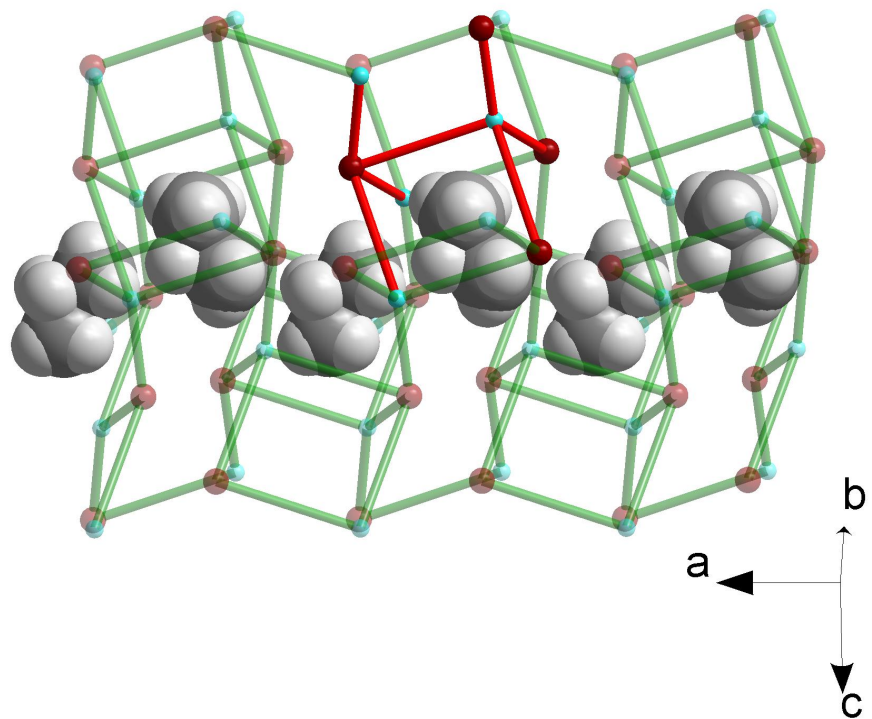


Figure S7. The ordered organic cation Me_2NH_2^+ resides in the cavity along the a -axis in LTP. The connected mode highlight in red and Me_2NH_2^+ highlight in space-filling mode.

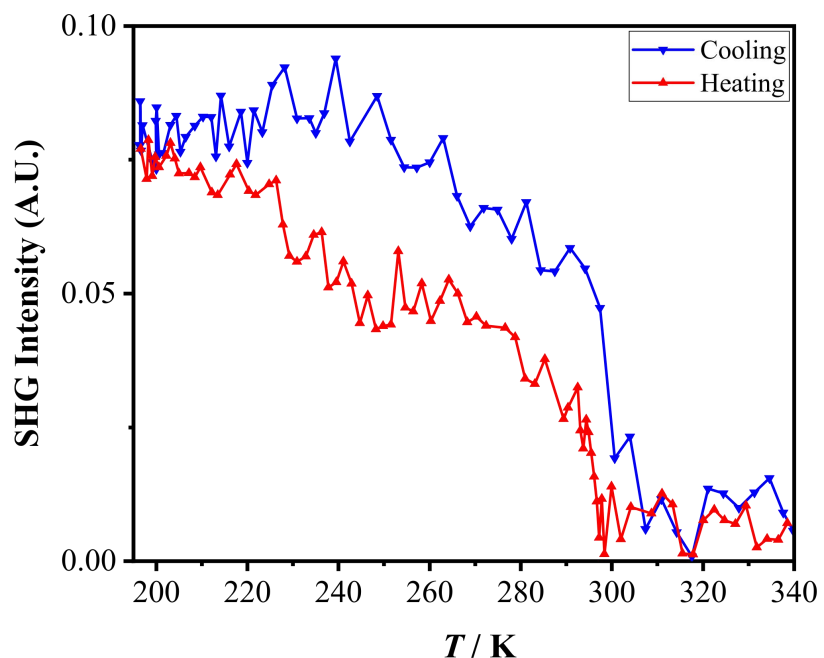


Figure S8. SHG signal curves of **1** upon cooling (blue) and heating (red).

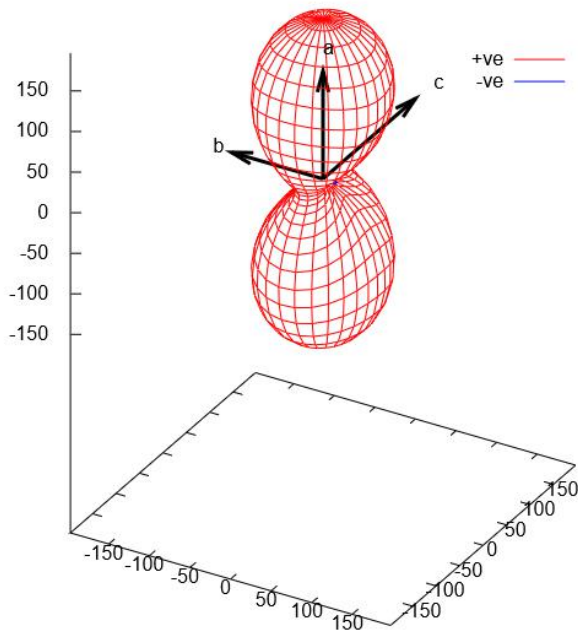


Figure S9. Expansivity indicatrix of **LTP** along the *a*, *b*, and *c* axes . NTE is shown in blue and PTE is shown in red.

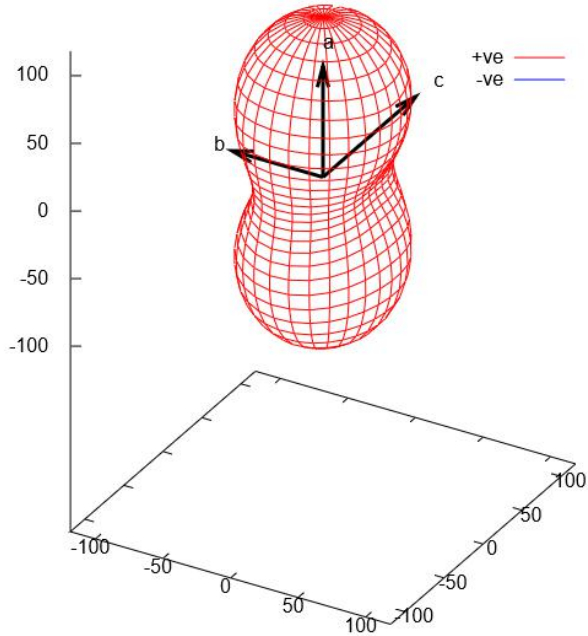


Figure S10. Expansivity indicatrix of **HTP** along the *a*, *b*, and *c* axes. NTE is shown in blue and PTE is shown in red.

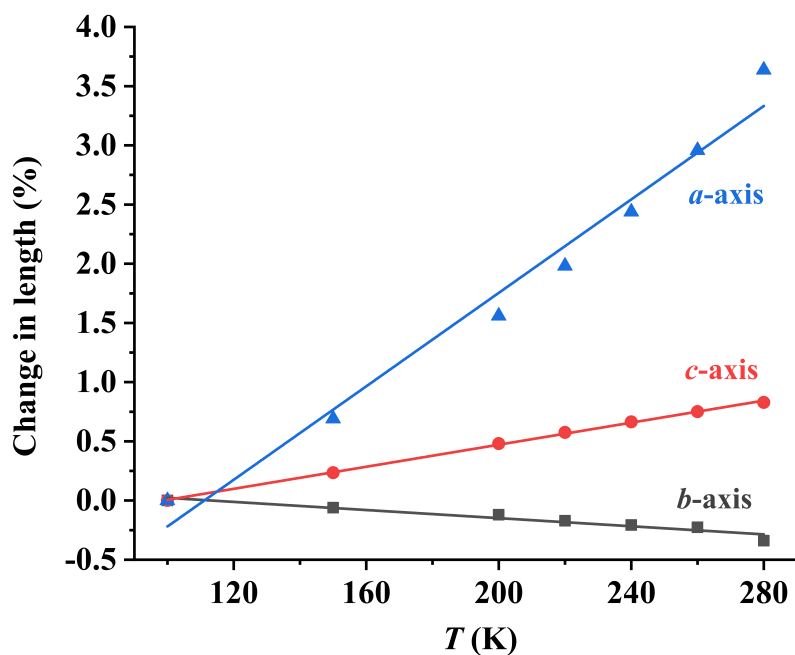


Figure S11. The percentage change of the cell parameters as a function of temperature in LTP, with lines of best fit.

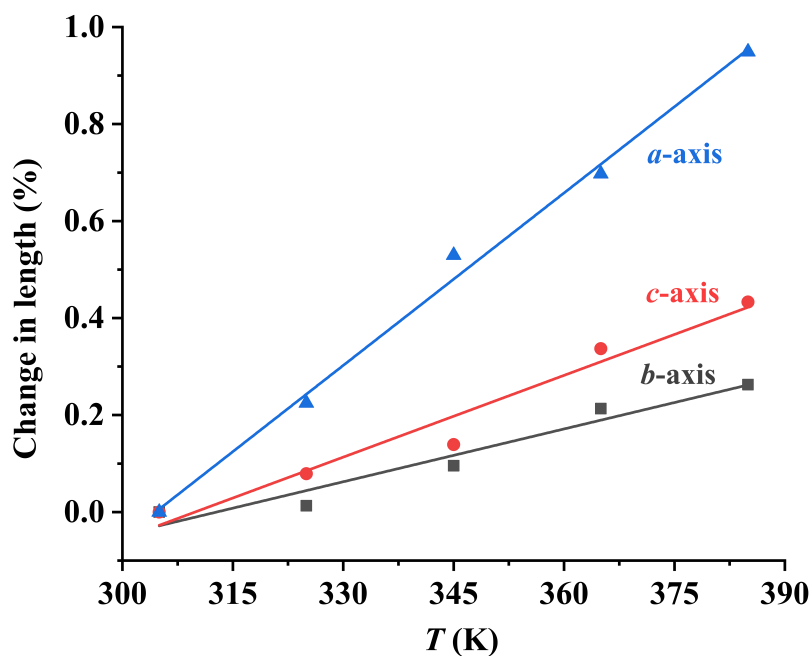


Figure S12. The percentage change of the cell parameters as a function of temperature in HTP, with lines of best fits.

References

- [S1] Sheldrick, G.M., *Acta Cryst.*, 2015, **A71**, 3-8.
- [S2] Dolomanov, O.V.; Bourhis, L.J.; Gildea, R.J.; Howard, J.A.K.; Puschmann, H., *J. Appl. Cryst.*, 2009, **42**, 339-341.
- [S3] C. Ji, Z. Sun, S. Zhang, S. Zhao, T. Chen, Y. Tang, J. Luo, *Chem. Commun.*, 2015, **51**, 2298-2300.
- [S4] T. Khan, M. Asghar, Z. Sun, A. Zeb, C. Ji, J. Luo *J. Mater. Chem. C*, 2017, **5**, 2865-2870.
- [S5] T. Chen, S. Sun, S. Zhao, C. Ji, J. Luo, *J. Mater. Chem. C*, 2016, **4**, 266-271.
- [S6] X. Chen, Y. Zhang, D. Sun, J. Gao, X. Hua, W. Liao, *Dalton. Trans.*, 2019, **48**, 11292-11297.
- [S7] W. Xu, Y. Zeng, W. Yuan, R. Qiu, W. Zhang, *Chem. Commun.*, 2018, **54**, 3347-3350.
- [S8] Z. Wu, X. Liu, C. Ji, L. Li, S. Wang, Z. Sun, W. Zhang, Y. Peng, J. Luo, *J. Mater. Chem. C*, 2018, **6**, 9532-9536.
- [S9] Z. Sun, T. Chen, C. Ji, S. Zhang, S. Zhao, M. Hong, J. Luo, *Chem. Mater.*, 2015, **27**, 4493-4498.
- [S10] S. Liu, Z. Sun, C. Ji, L. Li, S. Zhao, J. Luo, *Chem. Commun.*, 2017, **53**, 7669-7672.
- [S11] J. Zhang, S. Han, X. Liu, Z. Wu, C. Ji, Z. Sun, J. Luo, *Chem. Commun.*, 2018, **54**, 5614-5617.
- [S12] G. Mei, H. Zhang, W. Liao, *Chem. Commun.*, 2016, **52**, 11135-11138.
- [S13] W. Liao, H. Ye, D. Fu, P. Li, L. Chen, Y. Zhang, *Inorg. Chem.*, 2014, **53**, 11146-11151.
- [S14] X. Liu, C. Ji, Z. Wu, L. Li, S. Han, Y. Wang, Z. Sun, J. Luo, *Chem. Eur. J.*, 2019, **25**, 2610-2615.
- [S15] Y. Liu, D. Wu, Z. Wang, Y. Zhang, *New J. Chem.*, 2017, **41**, 3211-3216.
- [S16] L. Li, Z. Sun, P. Wang, W. Hu, S. Wang, C. Ji, M. Hong, J. Luo, *Angew. Chem. Int. Ed.*, 2017, **56**, 12150-12154.
- [S17] Z. Sun, X. Liu, T. Khan, C. Ji, M. A. Asghar, S. Zhao, L. Li, M. Hong, J. Luo, *Angew. Chem. Int. Ed.*, 2016, **55**, 6545-6550.
- [S18] Z. Wu, C. Ji, L. Li, J. Kong, Z. Sun, S. Zhao, S. Wang, M. Hong, J. Luo, *Angew. Chem. Int. Ed.*, 2018, **57**, 8140-8143.
- [S19] W. Liao, Y. Zhang, C. Hu, J. Mao, H. Ye, P. Li, S. Huang, R. Xiong, *Nat. Commun.*, 2015, **6**, 7338-7344.
- [S20] F. Geng, L. Zhou, P. Shi, X. Wang, X. Zheng, Y. Zhang, D. Fu, Q. Ye, *J. Mater. Chem. C*, 2017, **5**, 1529-1536.
- [S21] L. Zhou, X. Zheng, P. Shi, Z. Zafar, H. Ye, D. Fu, Q. Ye, *Inorg. Chem.*, 2017, **56**, 3238-3244.